J. Fluid Mech. (2011), *vol.* 668, *pp.* 436–445. © Cambridge University Press 2011
doi:10.1017/S0022112010005859

Inertial effects on viscous fingering in the complex plane

ANDONG HE[1]† AND ANDREW BELMONTE[1,2]

[1]W. G. Pritchard Laboratories, Department of Mathematics, The Pennsylvania State University, University Park, PA 16802, USA

[2]Department of Materials Science and Engineering, The Pennsylvania State University, University Park, PA 16802, USA

(Received 30 July 2010; revised 28 September 2010; accepted 9 November 2010)

We present a nonlinear unsteady Darcy's equation which includes inertial effects for flows in a porous medium or Hele-Shaw cell and discuss the conditions under which it reduces to the classical Darcy's law. In the absence of surface tension we derive a generalized Polubarinova–Galin equation in a circular geometry, using the method of conformal mapping. The linear stability of the base-flow state is examined by perturbing the corresponding conformal map. We show that inertia always has a tendency to stabilize the interface, regardless of whether a less viscous fluid is displacing a more viscous fluid or vice versa.

Key words: fingering instability, pattern formation

1. Introduction

Understanding the evolution of the interface between two immiscible fluids when one is flowing into the other is of fundamental importance in fluid dynamics. In a fluid held between two closely spaced parallel plates, known as a Hele-Shaw cell (Hele-Shaw 1899), if the displacing fluid has lower viscosity than the displaced fluid the interface will develop hydrodynamical instability which results in highly ramified patterns (Saffman & Taylor 1958; Paterson 1981; Bensimon 1986). This phenomenon is known as viscous fingering, and it may also occur when the elasticity of the fluids acts as another driving mechanism (Lemaire *et al.* 1991; Podgorski *et al.* 2007; Mora & Manna 2010). Pattern formation of similar type has been observed in a variety of non-equilibrium systems besides viscous fingering, such as crystal growth (Langer 1980), electrodeposition (Matsushita *et al.* 1984) and solidification (Hunt 1999).

The canonical mathematical model for Hele-Shaw flows is Darcy's law, where the flow velocity is proportional to the pressure gradient. Under the assumption that the flow is incompressible, the pressure field satisfies Laplace's equation; therefore, such an evolution of the free interface is also called the Laplacian growth process. By averaging the velocity over the direction perpendicular to the cell, one can reduce the three-dimensional flow problem to two-dimensional, thus allowing the use of complex variable techniques. As a powerful tool for both analysis (Bensimon 1986; Howison 1992) and numerical computations (Aitchison & Howison 1985; Dai *et al.* 1991),

† Email address for correspondence: he@math.psu.edu

https://doi.org/10.1017/S0022112010005859 Published online by Cambridge University Press

the method of conformal mapping takes its strength from transforming the generally difficult task of solving a moving-free boundary problem into finding solutions to a single differential equation of an analytic function on a fixed domain, usually the half-plane or the interior of the unit disk. Translating the dynamics implicit in Darcy's law to this formalism leads to an equation of the map for Hele-Shaw flows, derived independently by Polubarinova-Kochina and Galin in 1945, now known as the Polubarinova–Galin (P–G) equation (Howison 1992). Several exact solutions to the P–G equation have now been obtained (see Gustafsson & Vasil'ev 2006 for a comprehensive overview). The linear stability analysis for radial fingering done by Paterson (1981) can also be obtained using the P–G equation, as shown below. In the two-phase Hele-Shaw flow problem, much less progress has been made, since in general it is difficult to find a conformal map which takes a region and its complement in the parametric plane onto the corresponding regions occupied by the two phases. Exact solutions are attainable only in some special cases (Howison 2000; Crowdy 2006).

Despite the richness of studies in quasi-static Hele-Shaw flows, little effort can be found in the literature to understand the character of fluids' inertia. The desire to answer this question manifests itself when a fluid is injected in a time-dependent, especially fast-oscillating manner. In a recent work, Li *et al.* (2009) showed experimentally and numerically that the interfacial Saffman–Taylor instability in a circular cell can be suppressed by pumping the fluid at a rate $Q(t) \sim t^{-1/3}$. Yet, the equation they considered is Darcy's law; thus the role that inertia of fluids plays remains veiled. Gondret & Rabaud (1997) and Ruyer-Quil (2001) took into consideration the inertial effects and generalized Darcy's law under slightly different assumptions. The equations they obtained are of the same type but have different coefficients. Chevalier *et al.* (2006) examined experimentally that in a linear Hele-Shaw cell the inertial effects can be significant if the displacing fluid has low viscosity, or large velocity, or if the cell thickness is large, that is, if the modified Reynolds number is not too small. They found that inertia has similar effects as capillary force in that they both tend to slow down and widen the fingers.

A complete treatment of the Hele-Shaw problem, one which could include inertial effects, is still lacking. It is the main goal of this paper to investigate how inertial effects may alter the structure of this mathematical system and particularly the stability of the free interface. Our aim is to provide a mathematical description on the basis of the conformal-mapping method to enhance our understanding of the full Hele-Shaw flow problem. The contents of this paper are as follows: in § 2 we present a dimensionless form of the generalized Darcy's equation and the conditions under which it reduces to Darcy's law. The method of conformal mapping that leads to a generalization of P–G equation is presented in § 3. The generalized P–G equation allows not only exact solutions but also a straightforward way to study the stability of the problem. Section 4 is devoted to examining the linear stability of the free interface when inertial effects are not negligible, by perturbing the conformal map obtained from § 3. In § 5 we discuss how small inertia would change the stability of the interface.

2. Derivation of the unsteady nonlinear Darcy's equation

We denote by ρ, $\boldsymbol{v}$ and P the dimensional fluid density, velocity field and pressure field in the three-dimensional space, respectively. Let ν be the kinematic viscosity. Consider in a Hele-Shaw cell the three-dimensional Navier–Stokes equation with the

https://doi.org/10.1017/S0022112010005859 Published online by Cambridge University Press

incompressibility condition:

$$\boldsymbol{v}_t + (\boldsymbol{v} \cdot \nabla)\boldsymbol{v} = -\frac{1}{\rho}\nabla P + \nu \Delta \boldsymbol{v}, \tag{2.1}$$

$$u_x + v_y + w_z = 0. \tag{2.2}$$

Let U be the characteristic horizontal flow speed, L the horizontal length scale and h the thickness of the cell. For a typical Hele-Shaw cell $h/L \ll 1$, so it follows from (2.2) that w is of the order of Uh/L; thus is assumed to be zero. Consequently the z-component equation of (2.1) implies that P is a function of x and y only (see e.g. Acheson 1990).

Dimensionless variables can be defined as follows:

$$\left.\begin{aligned} (x', y', z') &= \frac{1}{L}\left(x, y, \frac{L}{h}z\right), \quad t' = \frac{t}{\tau}, \\ (u', v') &= \frac{1}{U}(u, v), \quad P' = \frac{h^2 P}{\rho \nu U L}. \end{aligned}\right\} \tag{2.3}$$

Using these variables and applying the lubrication approximation ($\Delta \boldsymbol{v} \simeq \partial^2 \boldsymbol{v}/\partial z^2$) we can rewrite (2.1) as

$$\alpha \hat{\boldsymbol{v}}_t + Re^*(\hat{\boldsymbol{v}} \cdot \nabla')\hat{\boldsymbol{v}} = -\nabla' P' + \frac{\partial^2 \hat{\boldsymbol{v}}}{\partial z'^2}, \tag{2.4}$$

where $\hat{\boldsymbol{v}} = (u', v')$ and $\nabla' = (\partial/\partial x', \partial/\partial y')$; $\alpha = h^2/\nu\tau$ is a dimensionless number and

$$Re^* = \frac{Uh^2}{\nu L} = \left(\frac{h}{L}\right) Re \tag{2.5}$$

is the modified Reynolds number (Chevalier *et al.* 2006). Since it can be inferred from (2.4) that when $\alpha = Re^* = 0$ the velocity $\hat{\boldsymbol{v}}$ has a parabolic profile, it is reasonable to assume that it remains parabolic when α and Re^* are small enough. In dimensionless form it reads

$$\hat{\boldsymbol{v}}(x', y', z', t') = z(z-1)\boldsymbol{A}(x', y', t'), \tag{2.6}$$

for $\boldsymbol{A} = (A_1, A_2)$. We define $\boldsymbol{u}'$ to be the averaged value of $\hat{\boldsymbol{v}}$,

$$\boldsymbol{u}'(x', y', t') \equiv \int_0^1 \hat{\boldsymbol{v}}(x', y', z', t')\, \mathrm{d}z', \tag{2.7}$$

and integrate (2.4) from $z = 0$ to $z = 1$. The resulting equation, with the primes dropped, is

$$\alpha \boldsymbol{u}_t + \tfrac{6}{5} Re^*(\boldsymbol{u} \cdot \nabla)\boldsymbol{u} + 12\boldsymbol{u} = -\nabla P. \tag{2.8}$$

The dimensional version of this equation was to our knowledge first derived by Gondret & Rabaud (1997). A similar approach was taken by Ruyer-Quil (2001), who obtained an equation in the same form but with different coefficients because of a discrepancy in the way the horizontal flow velocities were averaged. Here we derive the same equation, using slightly looser assumptions than Gondret & Rabaud (1997); namely the horizontal velocities have a more general form (as in (2.6)). Throughout this paper, (2.8) (with possibly different constant coefficients) will be called the unsteady nonlinear Darcy's (UND) equation.

Our derivation assumes that α and Re^* are both small. It is evident from (2.8) that Darcy's law is a limiting case of the UND equation when both α and Re^* vanish. In most experiments performed in Hele-Shaw cells, α and Re^* are small. Note that

https://doi.org/10.1017/S0022112010005859 Published online by Cambridge University Press

the Reynolds number $Re = Uh/\nu$ is not necessarily small. In order to understand the physical meaning of α, let us consider a viscous fluid being pumped into or removed from a cell through a point at a rate of area change:

$$Q(t) = Q_0 + Q_p \sin(\omega t) \tag{2.9}$$

(Q_0, Q_p and ω are constants). Fluid injection will correspond to $Q > 0$ and extraction to $Q < 0$; we require $|Q_p| < |Q_0|$ to avoid a scenario that includes both. Let $a(t)$ be the radius of the radially growing (or shrinking) interface; then it follows from mass conservation that

$$a(t) = \sqrt{\int_0^t \frac{Q}{\pi}\,\mathrm{d}s + a(0)^2}, \quad a(0) \geqslant 0. \tag{2.10}$$

The time scale τ can be defined to be the minimal value of the ratio of velocity of the growing circle to its acceleration within a period of oscillating injection:

$$\tau \sim \min_{t\in[t_0,t_0+\frac{2\pi}{\omega}]} \left|\frac{\dot{a}}{\ddot{a}}\right| = \min_{t\in[t_0,t_0+\frac{2\pi}{\omega}]} \left|\frac{\omega Q_p \cos(\omega t)}{Q} - \frac{Q}{2\pi a^2}\right|^{-1}. \tag{2.11}$$

Two distinct cases are worth emphasizing: (i) $Q_p = 0$, implying $\tau \sim 2t_0 + 2\pi a(0)^2/Q_0$. No second time scale thus exists, and choosing $\tau = L/U$ identifies α with Re^*. (ii) $Q_p \neq 0$ and ω is large. The dominant term in the absolute value sign of (2.11) is ω, so τ can be chosen to be $1/\omega$. We can infer from the second case that a rapid oscillation in the injection will invalidate Darcy's law.

3. Conformal-mapping approach

In this section we set up an equation to describe the motion of the free interface including inertial effects, by using the conformal-mapping method. The equation we derive is analogous to the P–G equation (Gustafsson & Vasil'ev 2006). The two-phase problem is notoriously difficult partly because the pressure is not constant on the interface. We will neglect the motion of the less viscous fluid so that the pressure conditions on the boundary are simplified, as discussed below. Consider a viscous fluid being injected into or removed from a Hele-Shaw cell from the origin at a time-dependent rate $Q(t)$. Motion of the flow is governed by the general dimensionless UND equation (cf. (2.8)):

$$\boldsymbol{u} + c_1 \boldsymbol{u}_t + c_2(\boldsymbol{u}\cdot\nabla)\boldsymbol{u} = -\nabla P, \tag{3.1}$$

where c_1, c_2 are positive constants. The flow is assumed to be incompressible and irrotational, so the velocity potential satisfies

$$\Delta\phi = Q(t)\delta(x), \tag{3.2}$$

for a Dirac delta distribution $\delta(x)$. We shall ignore surface tension effects and assume that the pressure is constant on $\Gamma(t)$; without loss of generality this constant can be taken to be zero. The second condition is that the material derivative of the pressure vanishes on $\Gamma(t)$, since it remains constant there. These two boundary conditions are written as

$$P = 0, \quad \frac{\mathrm{D}P}{\mathrm{D}t} = 0, \quad \text{on } \Gamma(t). \tag{3.3}$$

Here $\mathrm{D}/\mathrm{D}t \equiv \partial/\partial t + (\boldsymbol{u}\cdot\nabla)$ is the material derivative.

https://doi.org/10.1017/S0022112010005859 Published online by Cambridge University Press

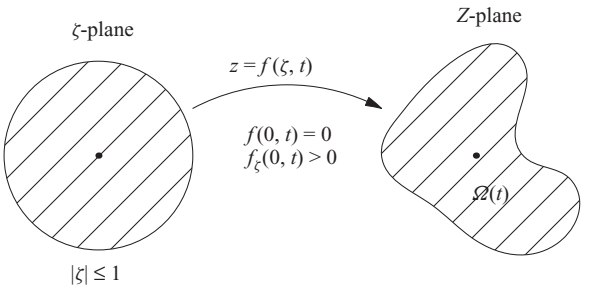


FIGURE 1. Sketch of the conformal map from the parametric ζ-plane to the physical Z-plane.

By the Riemann mapping theorem there exists a unique conformal univalent map $f(\zeta, t)$ from the unit disk in the (parametric) ζ-plane to the fluid region $\Omega(t)$ in the (physical) Z-plane such that $f(0, t) = 0$ and $f_\zeta(0, t) > 0$ (see figure 1). We denote by $F(z, t)$ the complex potential in the Z-plane with the real part ϕ; then the complex potential in the ζ-plane, $G(\zeta, t)$, is related to $F(z, t)$ via the time-dependent conformal map $f(\zeta, t)$ as

$$G(\zeta, t) = F(f(\zeta, t), t) = F(z, t). \tag{3.4}$$

We further assume that ϕ vanishes on $\Gamma(t)$; this condition with (3.2) determines that $G(\zeta, t) = Q(t)/2\pi \log \zeta + \mathrm{i}\kappa$ (κ is any real constant).

We write (3.1) as a Bernoulli-like equation

$$P = -\left(\phi + c_1\phi_t + \frac{c_2}{2}|\nabla\phi|^2\right) + H(t), \tag{3.5}$$

for some function H of t only. Since both ϕ and P are zero on $\Gamma(t)$, $H(t)$ should satisfy a compatibility condition given by the base flow state – a growing disk with the radius given by (2.10). That is,

$$H(t) = \left(c_1\phi_{0t} + \frac{c_2}{2}|\nabla\phi_0|^2\right)|_{\Gamma(t)} = \frac{Q^2}{8\pi^2 a^2}(c_2 - 2c_1), \tag{3.6}$$

where ϕ_0 is the potential for the base flow.

Substituting (3.5) into boundary conditions (3.3) we obtain

$$\phi_t + c_1\phi_{tt} + (c_1 + c_2)\nabla\phi\cdot\nabla\phi_t + |\nabla\phi|^2 + \frac{c_2}{2}\nabla\phi\cdot\nabla|\nabla\phi|^2 = \dot{H}(t) \quad \text{on} \quad \Gamma(t). \tag{3.7}$$

This equation can be rewritten in terms of f and its partial derivatives (see the Appendix):

$$\begin{aligned}\mathrm{Re}\left[-\frac{Qf_t}{2\pi\zeta f_\zeta} + \frac{c_1 Q}{2\pi}\left(\frac{2\zeta f_\zeta f_t f_{\zeta t} - \zeta f_\zeta^2 f_{tt} - \zeta f_t^2 f_{\zeta\zeta} - f_\zeta f_t^2}{\zeta^2 f_\zeta^3}\right) - \frac{c_1\dot{Q} f_t}{\pi\zeta f_\zeta} + \frac{(c_1 + c_2)Q\dot{Q}}{4\pi^2|f_\zeta|^2}\right.\\ \left. - \frac{(c_1 + c_2)Q^2}{4\pi^2}\left(\frac{\zeta f_\zeta f_{\zeta t} - \zeta f_t f_{\zeta\zeta} - f_t f_\zeta}{\zeta|f_\zeta|^2 f_\zeta^2}\right) - \frac{c_2 Q^3}{8\pi^3}\left(\frac{f_\zeta + \zeta f_{\zeta\zeta}}{f_\zeta|f_\zeta|^4}\right) + \frac{Q^2}{4\pi^2|f_\zeta|^2}\right]\\ = (c_2 - 2c_1)\left(\frac{Q\dot{Q}}{4\pi^2 a^2} - \frac{Q^3}{8\pi^3 a^4}\right), \quad \text{on} \quad |\zeta| = 1.\end{aligned} \tag{3.8}$$

We call this the generalized P–G equation. Note that c_1 and c_2 characterize respectively the magnitude of the time-derivative term and that of the convection term in the

https://doi.org/10.1017/S0022112010005859 Published online by Cambridge University Press

UND equation. When they are both zero, (3.8) reduces to the P–G equation

$$\mathrm{Re}\left[\zeta f_\zeta \overline{f_t}\right] = \frac{Q}{2\pi}, \tag{3.9}$$

whose many exact solutions in simple mappings such as polynomials and rational and logarithmic functions have been obtained (Howison 1986; Dawson & Mineev-Weinstein 1998; Gustafsson & Vasil'ev 2006). For example, if we assume

$$f(\zeta, t) = \beta_0(t)\zeta + \sum_{k=1}^{N} \beta_k(t) \log(\zeta - \gamma_k(t)) \tag{3.10}$$

($\beta_k(t)$, $\gamma_k(t)$ are complex functions), we obtain a system of ordinary differential equations in $\beta_k(t)$ and $\gamma_k(t)$, leading to a logarithmic solution. It is likely that other solutions to (3.8) can be found similarly.

4. Linear stability via conformal mapping

The task of determining the shape of the interface is equivalent to the search for conformal maps satisfying the generalized P–G equation (3.8). We wish to consider the linear stability of the base-flow solution $f_0(\zeta, t) = a(t)\zeta$ to infinitesimal two-dimensional disturbances. Any such disturbance, if assumed to be geometrically simply connected, can be represented as the image of the unit disk $|\zeta| \leqslant 1$ under some conformal map. Since the set of all polynomials $\{\zeta_k\}_{k=0}^{\infty}$ forms a basis for all analytic functions in $|\zeta| \leqslant 1$, we can consider the perturbed map corresponding to the nth mode:

$$f(\zeta, t) = a(t)\zeta + \epsilon b(t)\zeta^{n+1} + O(\epsilon^2), \tag{4.1}$$

where $\epsilon \ll 1$, and the real-valued function $b(t)$ is the perturbation function. A similar approach has been taken by Meiron *et al.* (1984) and Crowdy & Cloke (2002) in studies of point vortices.

As a test problem, we consider the P–G equation with non-zero surface tension (cf. Gustafsson & Vasil'ev 2006):

$$\mathrm{Re}[\zeta f_\zeta \overline{f_t}] = \frac{Q}{2\pi} + \gamma \mathscr{H}\left[\mathrm{i}\,\mathrm{Im}\frac{\zeta^2 S_f(\zeta, t)}{|f_\zeta|}\right](\theta), \quad \zeta = \mathrm{e}^{\mathrm{i}\theta}, \tag{4.2}$$

where $\mathscr{H}$ is the Hilbert transform,

$$\mathscr{H}[\psi](\theta) = \frac{1}{\pi}\mathrm{PV}\int_0^{2\pi} \frac{\psi(\mathrm{e}^{\mathrm{i}\theta'})}{1 - \mathrm{e}^{\mathrm{i}(\theta-\theta')}}\,\mathrm{d}\theta', \tag{4.3}$$

(PV denotes the Cauchy principal value), and $S_f(\zeta, t)$ is the Schwarzian derivative,

$$S_f(\zeta) = \frac{\partial}{\partial\zeta}\left(\frac{f_{\zeta\zeta}(\zeta, t)}{f_\zeta(\zeta, t)}\right) - \frac{1}{2}\left(\frac{f_{\zeta\zeta}(\zeta, t)}{f_\zeta(\zeta, t)}\right)^2. \tag{4.4}$$

Plugging (4.1) into (4.2) and equating the $O(\epsilon)$ terms yields

$$\dot{b}(t) = -\frac{(n+1)}{a^2}\left(\frac{Q}{2\pi} + \frac{n(n-1)\gamma}{a}\right) b(t). \tag{4.5}$$

Paterson (1981) obtained the above equation by applying the standard linear stability analysis. Here we recovered his result from the perspective of conformal-mapping perturbation. Note that when $\gamma = 0$ the interface is always stable (unstable) if

https://doi.org/10.1017/S0022112010005859 Published online by Cambridge University Press

$Q > 0$ ($Q < 0$). For $Q < 0$ the unstable interface is sensitive to perturbations of all wavelengths; moreover, those with the shortest wavelength have the fastest growth rate. When surface tension is present, it suppresses the growth of the disturbance with small wavelength, as expected (McLean & Saffman 1980; Paterson 1981).

With inertia included, we can perturb the conformal-map solution corresponding to the base-state flow as described above. An oscillating injection rate (2.9) is considered first. For convenience, we take $\alpha = Re^*$; thus $c_2 = (6/5)c_1$. Substituting (4.1) into (3.8) and equating the $O(\epsilon)$ terms yield the differential equation

$$c_1\ddot{b}(t) + p(t)\dot{b}(t) + q(t)b(t) = 0, \quad t \geqslant 0, \tag{4.6}$$

where $p(t)$ and $q(t)$ are given by

$$\left.\begin{aligned} p(t) &= 1 + \frac{(n-10)c_1 Q}{10\pi a^2} + \frac{2c_1\dot{Q}}{Q}, \\ q(t) &= (n+1)\left[\frac{Q}{2\pi a^2} + \frac{3c_1\dot{Q}}{2\pi a^2} - \frac{17c_1 Q^2}{20\pi^2 a^4}\right]. \end{aligned}\right\} \tag{4.7}$$

When $Q > 0$, we can show that the solution $b(t) \equiv 0$ is asymptotically stable in the sense of Lyapunov for small enough c_1; that is, $b(t) \to 0$ as $t \to \infty$. To see this, we define a (positive-definite) Lyapunov function

$$V(b, \dot{b}, t) = b^2 + c_1 b\dot{b} + \frac{c_1(2-p)}{2q}\dot{b}^2, \tag{4.8}$$

which bounds b^2 (up to a scalar factor), and show that $\lambda\dot{V} + q(t)V \leqslant 0$ for a large constant λ. Then since $\int_0^t q(\tau)\,\mathrm{d}\tau \to \infty$ as $t \to \infty$, it follows that $V \to 0$ as $t \to \infty$. This direct proof by construction fails if c_1 is larger than the critical value $\hat{c}_1 = (1/3\omega)\sqrt{(Q_0^2 - Q_p^2)/Q_p^2}$, since $q(t)$ then no longer remains positive for large t. In fact, for $c_1 > \hat{c}_1$, $q(t)$ has infinitely many zeros. Yet numerical computations indicate that $b(t)$ converges to zero for large c_1 as well (e.g. for $\hat{c}_1 = 0.05$, we find that $b \to 0$ for c_1 as large as 10).

5. Effects of small inertia on the linear stability: Wentzel–Kramers–Brillouin approximation

We next investigate how the linear stability results obtained by Paterson (1981) are changed by a small amount of inertia. In the following we will assume that the constant c_1 appearing in (4.6) is small and positive. It is known that the only boundary layer of (4.6) lies near $t = 0$ (Bender & Orszag 1978). We are more concerned with the behaviour of the solution at large time, in particular the convergence rate of the solution to zero as time approaches infinity. Using the Wentzel–Kramers–Brillouin approximation, we can assume that the outer solution of (4.6) takes the form

$$b_{out}(t) = \mathrm{e}^{g(t)}, \quad \text{where} \quad g(t) = g_0(t) + c_1 g_1(t) + O\left(c_1^2\right) \qquad (0 < c_1 \ll 1). \tag{5.1}$$

By substituting the above expression into (4.6) and equating the coefficients of $O(c_1^k)$ terms (notice that both $p(t)$ and $q(t)$ contain c_1), we obtain

$$b_{out}(t) = K \cdot \exp\left[-\int_0^t \frac{(n+1)Q}{2\pi a^2} + c_1 D_1(t) + O\left(c_1^2\right)\right], \tag{5.2}$$

https://doi.org/10.1017/S0022112010005859 Published online by Cambridge University Press

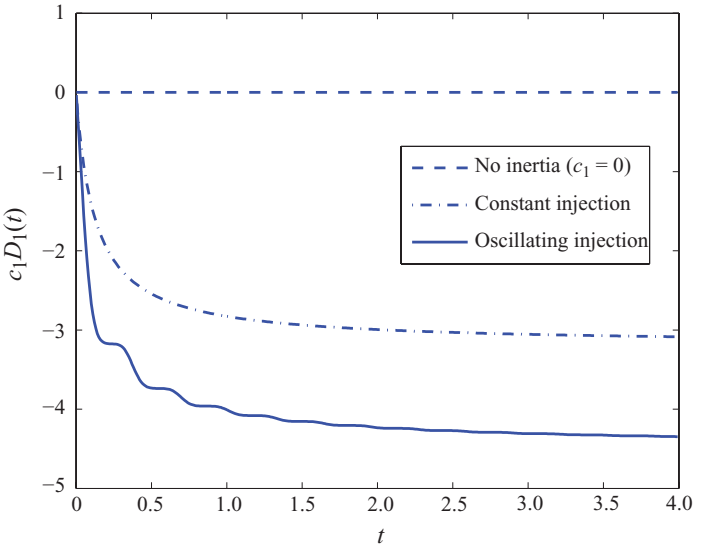


FIGURE 2. (Colour online) Plot of the function $c_1 D_1(t)$: the injection rate is (2.9) with $Q_0 = 1$, $Q_p = 0.8$, $\omega = 20$, $a(0) = 0.2$, $c_1 = 0.1$, $n = 3$.

where

$$D_1(t) = -\int_0^t \frac{(n+1)(n+2)Q^2}{5\pi^2 a^4}, \tag{5.3}$$

and the constant K is determined by asymptotic matching between the outer and inner solutions whose exact value is of little interest to us in the current study.

When $c_1 = 0$, $b_{out}(t) = \exp\{-\int_0^t (n+1)Q/2\pi a^2\}$ which reduces to the classical case of (4.5) for $\gamma = 0$. Note that the term $c_1 D_1(t)$ should be regarded as the inertial correction to the growth rate of the nth-mode perturbation. One can observe that $D_1(t) < 0$. It follows that small inertia always decreases the amplitude of the perturbation regardless of the direction of motion of the interface. This is in agreement with the experimental finding of Chevalier *et al.* (2006) that inertia tends to slow down the fingers. With an oscillating injection, the stability of the interface might be further enhanced by proper choice of the parameters in $Q(t)$ (see figure 2).

6. Conclusion

In this paper we have investigated the limits and corrections that inertia imposes on Darcy's law in a circular Hele-Shaw cell; we have found that it becomes invalid if either the modified Reynolds number is not small, or the frequency of the fluid injection is large. To describe the evolution of the free interface, we have applied the method of conformal mapping to derive a nonlinear non-local equation on the unit circle which takes into account inertial effects, a generalization of the P–G equation. It has been assumed that the interface is a level curve of the velocity potential. Since the pressure field is no longer harmonic, most methods developed to solve the Laplacian growth problem will not apply in this case. In particular, since (4.2) requires solving the Dirichlet problem for a harmonic function P, we have not been able to treat both inertial and surface tension effects in our formulation. The linear stability of the

https://doi.org/10.1017/S0022112010005859 Published online by Cambridge University Press

base-state solution, a uniformly growing circle whose radius depends on the injection rate, has been analysed by perturbing the corresponding conformal map.

If the inertia is small but not negligible, we have shown that it contributes only a secondary effect and does not change the Saffman–Taylor instability drastically. Moreover, whether a less viscous fluid displaces a more viscous fluid or vice versa, small inertia always has the tendency to stabilize, in that the amplitude of the disturbance approaches zero faster than the non-inertial case. This stabilizing tendency can be further enhanced by proper choice of the injecting function $Q(t)$. When the inertia is large, no rigorous conclusion has been drawn; yet numerical computations suggest the same stabilizing effect.

The scenario we have examined here is for a Hele-Shaw flow in a circular geometry, with a viscous fluid injected or extracted at one point. One can extend this analysis to the situation in which a viscous fluid sits at the exterior and a less viscous one is injected or extracted at a point and also to a cell with linear geometry.

Appendix. Derivation of the generalized Polubarinova–Galin equation (3.8)

Taking partial derivatives of (3.4) with respect to z and t and using $\zeta_t = -f_t/f_\zeta$ we can compute

$$\left.\begin{aligned}
&F_z = \frac{Q}{2\pi\zeta f_\zeta}, \quad F_t = \frac{\dot{Q}}{2\pi}\log\zeta + \frac{Q}{2\pi} = \frac{\dot{Q}}{2\pi}\log\zeta - \frac{Qf_t}{2\pi\zeta f_\zeta},\\
&F_{tz} = \frac{\partial F_t}{\partial\zeta}\Big/\frac{\partial z}{\partial\zeta} = \frac{\dot{Q}}{2\pi\zeta f_\zeta} - \frac{Q}{2\pi}\frac{\zeta f_\zeta f_{\zeta t} - \zeta f_t f_{\zeta\zeta} - f_t f_\zeta}{\zeta^2 f_\zeta^3},\\
&F_{tt} = \frac{\partial}{\partial t}F_t + \frac{\partial}{\partial\zeta}F_t\cdot\zeta_t = \frac{\ddot{Q}}{2\pi}\log\zeta - \frac{\dot{Q}f_t}{\pi\zeta f_\zeta} + \frac{Q}{2\pi}\frac{2\zeta f_\zeta f_t f_{\zeta t} - \zeta f_\zeta^2 f_{tt} - \zeta f_t^2 f_{\zeta\zeta} - f_\zeta f_t^2}{\zeta^2 f_\zeta^3},\\
&F_{zz} = \frac{\partial}{\partial\zeta}F_z/f_\zeta = -\frac{Q}{2\pi}\frac{f_\zeta + \zeta f_{\zeta\zeta}}{\zeta^2 f_\zeta^3}.
\end{aligned}\right\} \tag{A 1}$$

To write the above equations in terms of the conformal map f and its partial derivatives, we first observe that from the definition of F we have

$$\phi_t = \mathrm{Re}(F_t) = -\mathrm{Re}\left(\frac{Qf_t}{2\pi\zeta f_\zeta}\right), \quad \phi_{tt} = \mathrm{Re}(F_{tt}), \quad |\nabla\phi|^2 = |F_z|^2 = \frac{Q^2}{4\pi^2|f_z|^2}. \tag{A 2}$$

Moreover, since $F_z = \phi_x - \mathrm{i}\phi_y$ and $F_{zt} = \phi_{xt} - \mathrm{i}\phi_{yt}$,

$$\begin{aligned}
\nabla\phi\cdot\nabla\phi_t &= \mathrm{Re}(\overline{F_z}F_{zt})\\
&= \mathrm{Re}\left(\frac{Q\dot{Q}}{4\pi^2|f_\zeta|^2} - \frac{Q^2}{4\pi^2}\frac{\zeta f_\zeta f_{\zeta t} - \zeta f_t f_{\zeta\zeta} - f_t f_\zeta}{\zeta|f_\zeta|^2 f_\zeta^2}\right).
\end{aligned} \tag{A 3}$$

Similarly, since

$$\nabla|\nabla\phi|^2 = (2\phi_x\phi_{xx} + 2\phi_y\phi_{xy}, 2\phi_x\phi_{xy} + 2\phi_y\phi_{yy}) = (2\,\mathrm{Re}(F_z\overline{F}_{zz}), 2\,\mathrm{Im}(F_z\overline{F}_{zz})), \tag{A 4}$$

the last term on the left-hand-side of (3.7) can be rewritten as

$$\begin{aligned}
\nabla\phi\cdot\nabla|\nabla\phi|^2 &= 2(\mathrm{Re}(\overline{F}_z), \mathrm{Im}(\overline{F}_z))\cdot(\mathrm{Re}(F_z\overline{F}_{zz}), \mathrm{Im}(F_z\overline{F}_{zz})) = 2\,\mathrm{Re}(F_z^2\overline{F}_{zz})\\
&= -\frac{Q^3}{4\pi^3}\frac{f_\zeta + \zeta f_{\zeta\zeta}}{f_\zeta|f_\zeta|^4}.
\end{aligned} \tag{A 5}$$

https://doi.org/10.1017/S0022112010005859 Published online by Cambridge University Press

The authors would like to express their gratitude to Darren Crowdy and Björn Gustafsson and especially to Mark Levi for many helpful discussions and suggestions. They also thank Harvey Segur and José Miranda for comments on the paper.

REFERENCES

Acheson, D. 1990 *Elementary Fluid Dynamics*. Oxford University Press.

Aitchison, J. & Howison, S. 1985 Computation of Hele-Shaw flows with free boundaries. *J. Comput. Phys.* **60**, 376–390.

Bender, C. & Orszag, S. 1978 *Advanced Mathematical Methods for Scientists and Engineers*. McGraw-Hill.

Bensimon, D. 1986 Stability of viscous fingering. *Phys. Rev.* A **33**, 1302–1308.

Chevalier, C., Amar, M., Bonn, D. & Lindner, A. 2006 Inertial effects on Saffman–Taylor viscous fingering. *J. Fluid Mech.* **552**, 83–97.

Crowdy, D. 2006 Exact solutions to the unsteady two-phase Hele-Shaw problem. *Q. J. Mech. Appl. Math.* **59**, 475–485.

Crowdy, D. & Cloke, M. 2002 Stability analysis of a class of two-dimensional multipolar vortex equilibria. *Phys. Fluids* **14**, 1862–1876.

Dai, W.-S., Kadanoff, L. & Zhou, S.-M. 1991 Interface dynamics and the motion of complex singularities. *Phys. Rev.* A **43**, 6672–6682.

Dawson, S. & Mineev-Weinstein, M. 1998 Dynamics of closed interfaces in two-dimensional Laplacian growth. *Phys. Rev.* E **57**, 3063–3072.

Gondret, P. & Rabaud, M. 1997 Shear instability of two-fluid parallel flow in a Hele-Shaw cell. *Phys. Fluids* **9** (11), 3267–3274.

Gustafsson, B. & Vasil'ev, A. 2006 *Conformal and Potential Analysis in Hele-Shaw Cells*, Birkhauser.

Hele-Shaw, H. S. 1899 The flow of water. *Nature* **59**, 222–223.

Howison, S. 1986 Fingering in Hele-Shaw cells. *J. Fluid Mech.* **167**, 439–453.

Howison, S. 1992 Complex variable methods in Hele-Shaw moving boundary problems. *Euro. J. Appl. Math.* **3**, 209–224.

Howison, S. 2000 A note on the two-phase Hele-Shaw problem. *J. Fluid Mech.* **409**, 243–249.

Hunt, J. 1999 Pattern formation in solidification. *Mater. Sci. Tech.* **15**, 9–15.

Langer, J. 1980 Instabilities and pattern formation in crystal growth. *Rev. Mod. Phys.* **52**, 1–28.

Lemaire, E., Levitz, P., Daccord, G. & Damme, H. 1991 From viscous fingering to viscoelastic fracturing. *Phys. Rev. Lett.* **67**, 2009–2012.

Li, S., Lowengrub, J., Fontana, J. & Palffy-Muhoray, P. 2009 Control of viscous fingering patterns in a radial Hele-Shaw cell. *Phys. Rev. Lett.* **102**, 174501.

McLean, J. & Saffman, P. 1980 The effect of surface tension on the shape of fingers in a Hele-Shaw cell. *J. Fluid Mech.* **102**, 455–469.

Matsushita, M., Sano, M., Hayakawa, Y., Honjo, H. & Sawada, Y. 1984 Fractal structures of zinc metal leaves grown by electrodeposition. *Phys. Rev. Lett.* **53**, 286–289.

Meiron, D., Saffman, P. & Schatzman, J. 1984 The linear two-dimensional stability of inviscid vortex streets of finite-cored vortices. *J. Fluid Mech.* **147**, 187–212.

Mora, S. & Manna, M. 2010 Saffman–Taylor instability of viscoelastic fluids: from viscous fingering to elastic fractures. *Phys. Rev.* E **81**, 026305.

Paterson, L. 1981 Radial fingering in a Hele-Shaw cell. *J. Fluid Mech.* **113**, 513–529.

Podgorski, T., Sostarecz, M. C., Zorman, S. & Belmonte, A. 2007 Fingering instabilities of a reactive micellar interface. *Phys. Rev.* E. **76**, 016202.

Ruyer-Quil, C. 2001 Inertial corrections to the Darcy law in a Hele-Shaw cell. *C. R. Acad. Sci., Paris* IIb **329**, 337–342.

Saffman, P. & Taylor, G. I. 1958 The penetration of a fluid into a porous medium or Hele-Shaw cell containing a more viscous fluid. *Proc. R. Soc. Lond.* A **245**, 312–329.

https://doi.org/10.1017/S0022112010005859 Published online by Cambridge University Press